Thin Solid Films 520 (2012) 6434–6439

Contents lists available at SciVerse ScienceDirect

Thin Solid Films

journal homepage: www.elsevier.com/locate/tsf

# Rationally designed porous silicon as platform for optical biosensors

G. Priano [a], L.N. Acquaroli [b], L.C. Lasave [b], F. Battaglini [a], R.D. Arce [b,c,*], R.R. Koropecki [b,c]

[a] INQUIMAE, DQIAyQF, FCEN, Universidad de Buenos Aires, Ciudad Universitaria, Pabellón 2 (C1428EHA) Buenos Aires, Argentina
[b] Instituto De Desarrollo Tecnologico Para La Industria Quimica, UNL, CONICET, Güemes 3450 (S3000GLN) Santa Fe, Argentina
[c] Departamento De Materiales, Facultad De Ingenieria Quimica, UNL, Santiago del Estero 2829 (S3000) Santa Fe, Argentina

ARTICLE INFO

*Article history:*
Received 23 September 2011
Received in revised form 13 June 2012
Accepted 14 June 2012
Available online 21 June 2012

*Keywords:*
Nanostructured porous silicon
Optical microcavity
Biosensors
Functionalization
Response simulation

ABSTRACT

Optical porous silicon multilayer structures are able to work as sensitive chemical sensors or biosensors based in their optical response. An algorithm to simulate the optical response of these multilayers was developed, considering the optical properties of the individual layers. The algorithm allows designing and customizing the porous silicon structures according to a given application. The results obtained by the simulation were experimentally verified; for this purpose different photonic structures were prepared, such as Bragg reflectors and microcavities. Some of these structures have been derivatized by the introduction of aminosilane groups on the porous silicon surface. The algorithm also permits to simulate the effects produced by a non uniform derivatization of the multilayer.



## 1. Introduction

Porous silicon (PS) becomes interesting for sensing applications due to its unique properties: large specific surface area (thousands times the surface of the polished silicon wafer), controllable pore sizes, appropriate surface chemical reactivity and its potential to be integrated to the conventional silicon technology. Optical and electrochemical sensors based in PS technology are also well-suited for label-free sensing [1–3].

PS can be prepared by electrochemical etching of silicon (Si) wafer using a fluorinated electrolyte. Under suitable fabrication conditions the process generates a pore network formed of nano- or microcrystalline domains with defined pore morphologies. The geometric shape and diameter of the pores depend on several parameters: the applied current density, the composition of the etching solution, the temperature of the reacting interface, and the characteristics of the silicon wafer (surface orientation, doping level and type of doping) [4]. Depending on the size of the pores, the material is usually classified as nanoporous (structures in the scale of 1 to 10 nm), mesoporous (structures in the scale of 10 to 100 nm) or macroporous (structures scaling up to the micrometers) [5].

The porous formation by anodization of silicon is a self-limited process. An arbitrary current versus time profile is transferred in a porous structure versus depth profile [4]. Consequently, it is possible to obtain a multilayer with specific optical response by changing the anodization parameters. Periodically alternated layers having the same optical thicknesses but different refractive indexes conforms a unidimensional photonic crystal called Distributed Bragg Reflector (DBR). The spectrum of such device presents a band of efficient reflectance (named stopping band or photonic band gap) around a wavelength equal to four times the optical thickness of each layer. The introduction of an appropriate defect breaks the symmetry of the structure generating an optical response that shows one or more narrow resonances in the stopping band. Such structure configures an optical microcavity in which the electromagnetic field is confined between two Bragg mirrors. These structures are susceptible to changes in the refractive index of the environment due to its porous characteristics, becoming appropriate optical sensors. When it is used for sensing purposes, the porous network characteristics are adjusted by choosing the proper anodization parameters, to allow the infiltration of analytes coming from the surrounding medium. The presence of these analytes may change the refractive indexes of each layer, changing the optical response of the whole multilayer. Thus, large changes in reflectance (or transmittance) at the original resonances wavelengths can be employed in sensing applications, providing an adequate ratio between the porous diameter and molecular size of the analyte.

Besides the sensitivity, the sensor also has selectivity requirements. The device can be made selective by modifying their surfaces in order to obtain a specific functionality. A prerequisite for using PS structures as optical sensors is the mechanical and chemical stability of the material under chemical treatments and handling in order to provide a reproducible response [6]. First, it is necessary to passivate the surface and to protect Si from solvent molecules and then, this surface must be appropriately modified to obtain the required functionality [7]. Commonly, the interaction between biomolecules, cells or tissues and materials is achieved by means of a stable intermediate layer containing a recognition agent. The

* Corresponding author at: Instituto De Desarrollo Tecnologico Para La Industria Quimica, UNL, CONICET, Güemes 3450 (S3000GLN) Santa Fe, Argentina. Tel.: +54 342 455 9190; fax: +54 342 455 0944.
*E-mail address:* rarce@intec.unl.edu.ar (R.D. Arce).

0040-6090/$ – see front matter 
doi:10.1016/j.tsf.2012.06.055

intermediate layer should provide adequate functional groups that will anchor a biomolecule for recognition purposes. The most common functional groups are –SH (thiols), $-NH_2$ (amines) and –COOH (carboxylic acids) that can be covalently bound to biomolecules through mild reactions, preserving their recognition features. Functionalization with 3-aminopropyl(triethoxy)silane (APTES) leads to the presence of amine groups on the surface. Amine groups are assiduously chosen as functional group because they are present in proteins and their chemical reactions with other functional groups are well characterized [8]. Consequently, it is important not only to provide derivatization methods that allow a reproducible modification of the surface, but also a simple way to establish the proper modification of the whole structure and its effect on the optical response. For this reason, a computer algorithm able to simulate the effect on the refractive index response due to the modification process is a useful tool in sensor's design.

The optical behavior of porous silicon structures can be described by a simple and effective model, the Looyenga–Landau–Lifshitz (LLL) approach [9–11]. In this approach, a PS layer is considered as a nanocomposite made of a silicon–air mixture, which behaves as a continuous medium, assuming the wavelength of incident light is larger than pore size. Therefore, knowing the dielectric functions of each component and within an isotropic effective medium approach, the reflectance of a single film is completely determined by its porosity and its thickness. However, the LLL model has some limitations when it is applied to the construction of biosensors, since the intermediate and the recognition element form a layer covering the pore network surface, and the dielectric function changes to unknown values. To overcome this problem, the real part of the refractive index can be thought to monotonically decrease with wavelength [12], considered from here onward, the monotonic approach. In summary, this point represents a different approach taking into account that there are not works dedicated to reproduce complete reflectance spectra on a basis of known relationship between porosity and refractive index, although other authors have partially used similar procedures but they were not formally described.

In this work, the rational design of photonic devices and the analysis in relation to the effectiveness of the chemical modification are presented. The design and its evaluation are based in the use of two computational codes developed on the previously described approaches and transfer matrix method [13]. The procedure involves the measurements of reflectance as a function of the wavelength for single PS layers prepared under different electrochemical conditions. From these measurements the complexes refractive indexes of single layers are obtained. Based on this information, PS devices were designed and produced. Then, two strategies for surface derivatization were also tested: the one step aminosilanization catalyzed by organic bases [14] and the chemical oxidation followed by derivatization with aminosilanes, carried out in two steps [15]. Finally, a new spectrum is taken and by applying the second algorithm the homogeneity of the modification can be established. The results presented here show the capacity of these algorithms to design optical PS devices and its ability to evaluate the chemically modified surfaces.

## 2. Experimental details

### 2.1. Preparation of PS samples

Single side polished p-type silicon wafers ($1–4\times10^{-3}\,\Omega$.cm), <100> oriented were used as starting material. The wafers were immersed in 20% aqueous HF for 10 min to remove the native oxide. Then, the surface was electrochemically etched in darkness in a 2:1 solution (v/v) of absolute ethanol and 50% aqueous HF. Different current densities were used in the range of 12.4 to 128 mA $cm^{-2}$, controlling the anodization time for each current density. A Teflon® cell was employed for this purpose, where the silicon was the anode and a platinum wire was the cathode. After etching, the samples were rinsed with ethanol and dried under $N_2$ gas flow.

### 2.2. Preparation of chemically modified PS samples

The freshly etched PS samples were modified by silanization applying two different procedures.

One step modification: The PS oxidation and aminosilanization were carried out in a single step. The silanization reaction is thought to be the hydrolysis of $Si–H_x$ species catalyzed by an organic base and then the abstraction of H from Si–OH with alkoxysilane [14]. The reagent was prepared as follows: 125 μL of APTES and 25 μL of triethylamine were added into 2.4 mL of toluene. This solution was added onto the PS surfaces and incubated for 30 min. Then, the solution was removed and the sample was rinsed with toluene and ethanol, and dried under $N_2$ gas flow. The modification reaction is shown in the scheme of Fig. 1a.

Two step modification: In this alternative procedure, freshly etched PS samples were first chemically oxidized by immersion in 30% hydrogen peroxide ($H_2O_2$) for a period of 48 h at room temperature. As a result, a very thin film of hydrophilic oxide is formed [15]. After oxidation, the samples were rinsed with deionized water and dried under $N_2$ gas flow. In a second step, the oxidized samples were incubated with a 5% APTES solution in toluene for 30 min. After that, they were rinsed with toluene and placed in a stove at 120 °C for 20 min. The modification reaction is shown in the scheme of Fig. 1b.

### 2.3. Reflectance measurements and optical properties determination

A fast and simple instrumental, a conventional UV–VIS spectrometer with a home made reflectance accessory, was used in order to obtain low angle reflectance spectra for the PS samples prepared in Sections 2.1 and 2.2 steps.

Porosities and thicknesses of single porous layers in Sections 2.1 and 2.2 stages were determined by fitting their reflectance spectra using different approaches, as will be described below. From the resulting data, the optical thicknesses were determined as a function of photon energy and the anodization time. In both cases, Sections 2.1 and 2.2, the optical thickness grow rate is defined as the quotient between the optical thickness and the corresponding anodization time.

## 3. Theoretical aspects

In order to rationally design PS photonic devices and to predict their optical responses, the energy resolved complex refractive index (or the complex dielectric function) and the optical thickness growth rate of the porous material have to be determined for each set of anodization conditions. These calculations were made by fitting the reflectance spectra of PS single layers prepared under different etching conditions, using the following approximations, according to chemical treatment on the samples surfaces.

### 3.1. Non-modified PS samples: Looyenga–Landau–Lifshitz (LLL) approach

Considering the porous silicon to be a nanocomposite with effective dielectric function $\varepsilon_{eff}$, the first component to be air ($\varepsilon_1=1$) with a volume fraction equal to the porosity $p$ and the second component to be Si ($\varepsilon_2$), the LLL approach predicts that the effective dielectric function is given by [4]

$$\varepsilon_{eff}^{1/3} = p\varepsilon_1^{1/3} + (1-p)\varepsilon_2^{1/3}. \quad (1)$$

The complex refractive index of porous silicon, $N_{eff}=n_{eff}+i\,k_{eff}$, is obtained as $\varepsilon_{eff}^{1/2}$. Therefore, by knowing the porosity, $\varepsilon_1$ and $\varepsilon_2$, $N_{eff}$ can be determined. The real part of $N_{eff}$ is the refractive index, $n_{eff}$, and the imaginary part is the extinction coefficient, $k_{eff}$.

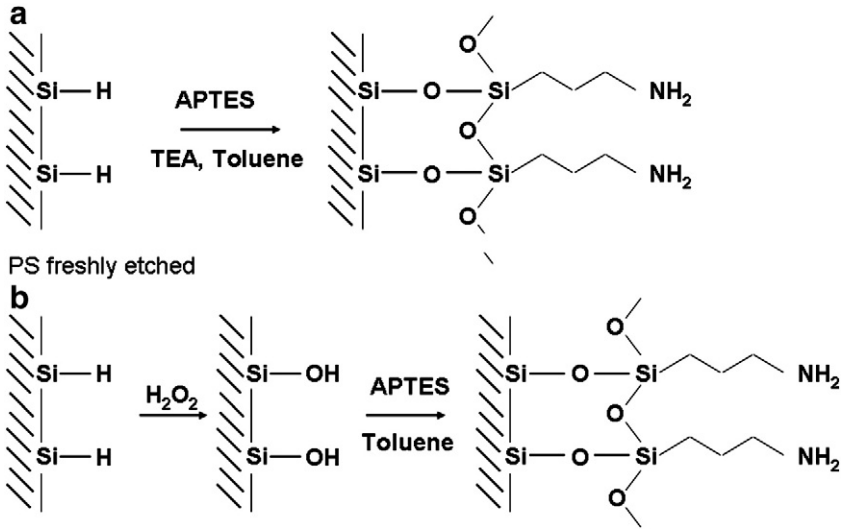


**Fig. 1.** Scheme of the pore surface modified by silanization: one step (1a) and two step procedure (1b).

A two stages algorithm was used to fit the reflectance spectra of single layers. In a first stage, a genetic algorithm [16] was used to provide initial estimations of the parameters, i.e. the porosity, $p$ and the thickness layer, $L$. These initial estimations served as seed parameters for a conventional [17] (Nelder–Mead) fitting algorithm in a second stage.

### 3.2. Modified PS samples: monotonic approach

When PS is derivatized for sensing purposes, a modified layer covers the pore network surface. As the dielectric function of such modified layer is unknown, no effective medium mixing rule can be employed to fit the reflectance spectra. In order to get over this problem, we proposed an alternative method assuming that the real part of the refractive index decreases monotonically with the wavelength [12]. In this case, the set of initialization parameters of the fitting algorithm is composed by 12 equally distributed values of $n_{eff}$ and $k_{eff}$ in a given interval of wavelengths. The thickness of the porous layer is also given as an initial parameter. The reflectance spectrum was reconstructed by using the refractive index and extinction coefficient obtained through spline approximations based on the parameters. Optimization was carried out as in the previous approach, with the two-stage algorithm described above.

Both approaches, LLL and monotonic, minimize a penalization function comparing the reconstructed reflectance spectrum with the experimental one.

### 3.3. Multilayer simulation

Once the refractive indexes and the thicknesses of PS single layers were determined, this information can be used to designed photonic structures with specific optical responses, and also to predict the effect of the analyte penetration inside the PS multilayers. Multilayers were simulated based on the well known optical transfer matrix method [13]. The developed simulation program predicts the reflectance spectrum for a given PS multilayer. For each wavelength, the optical transference matrix of the PS stack can be computed as the product of the transference matrixes of the individual layers. The method [12,18] provides a relationship between the incident electric field in the input side of the stack and that of the output side, consequently, a simple energetic balance allows the calculation of the reflectance spectrum.

## 4. Results and discussion

Fig. 2 shows the result of the fitting of the reflectance for a non modified sample using the LLL approach. The solid line corresponds to the experimental result while the dots represent the result of the fitting. Once the porosity is obtained, the refractive index and the extinction coefficient may be evaluated for each sample with Eq. (1).

Fig. 3 describes schematically how a computational code seeded with a few experimental results can be used to predict the density current and time conditions to build a layer with an optical response at a given wavelength $\lambda_c$. First, reflectance spectra for single layer PS samples are measured for each experimental anodization condition and then, they are fitting using the appropriated approach. Fig. 3a shows the experimental spectra (solid line) obtained for an APTES modified sample prepared with a current density of 12.4 mA $cm^{-2}$, for 62 s. The result of the fitting (full square symbols) using the monotonic approach is also shown in the same figure. As result of the fitting, the refractive index and the extinction coefficient of the different samples are evaluated as a function of the wavelength. These calculated values are plotted in Fig. 3b for the data recorded in Fig. 3a. Finally, combining the refractive index data and the thickness resulting from the above detailed fitting procedures, the time required to get a layer of an optical thickness equal to $\lambda_c/4$ can be obtained for all wavelengths, where $\lambda_c$ is the specific wavelength at

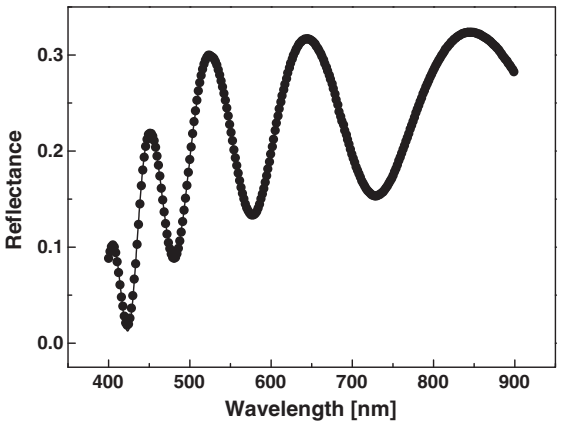


**Fig. 2.** Measured reflectance spectra of a non modified sample (solid line). The dots correspond to the fitting of these data using the Looyenga–Landau–Lifshitz model, with the porosity as the only free parameter.

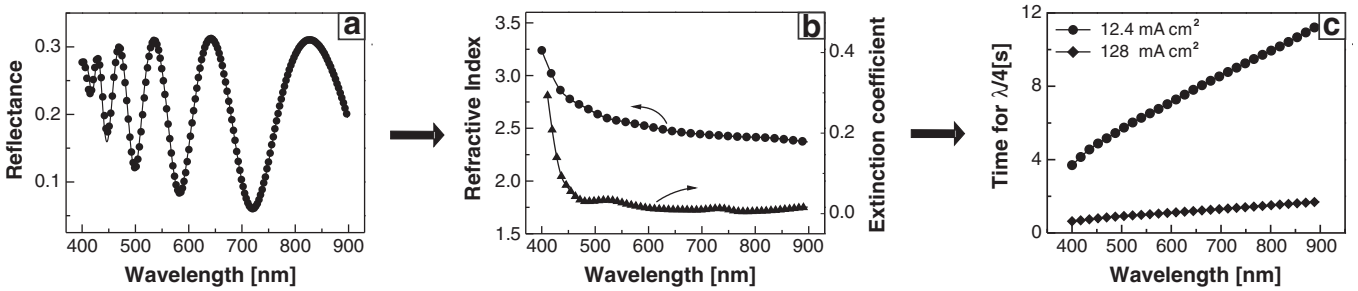


**Fig. 3.** Scheme showing how the experimental spectra and the computational codes are used for the construction of the PS structures. In this example, the measured reflectance spectra of a APTES modified single layer is presented. The layer was obtained using an anodization current density of 12.4 mA $cm^{-2}$ for 62 s (solid line). These results, together with the fitting obtained using the parametric approach (dots) are recorded in (a). In (b), the refractive index and the extinction coefficient obtained by the fitting of the reflectance spectrum of a single layer of PS in (a) are plotted as a function of the wavelength. The necessary times to etch a PS film with an optical thickness of λ/4 are represented in (c). These curves are obtained combining the results for different current densities and times. The different curves correspond to different current densities; the upper curve correspond to 12.4 mA $cm^{-2}$ and the lower to 128 mA $cm^{-2}$.

which the multilayer structure has the desired optical response. Fig. 3c shows the result of this combination. Notice that each curve in the figure comes from an experimentally recorded spectrum for a sample obtained at a particular current density and anodization time. The anodization time necessary to grow a modified film of $\lambda_c/4$ optical thickness is plotted in this figure as a function of the wavelength for two different anodization current densities: 128 mA $cm^{-2}$ and 12.4 mA $cm^{-2}$. In other words, for each current density, the time needed to obtain a layer with a given optical thickness can be obtained from the graph. In this way, for a given optical thickness, a combination of current density and refractive index can be obtained. From this set of parameters, two conditions are chosen to build a structure formed by alternated low and high porosity layers. For example, under this conditions, to obtain a photonic structure with response at $\lambda_c = 700$ nm, current densities of 12.4 and 128 mA.$cm^{-2}$ needs to be used in the anodization process, for 8.6 s and 1.3 s, respectively.

Therefore, once the growth rate of the chemically modified porous layers, as well as complex refractive indexes for different growing conditions, were obtained from the corresponding reflectance spectra, it was possible to design the desired multilayer with a given optical response showing that the construction of these graphs allows obtaining an optimized set of applicable experimental conditions in order to rationally design structures that fulfill established requirements, such as the wavelength of operation of the sensor, refractive index, etc.

Similarly, to simulate the optical response of a non modified sample, the procedure can be repeated starting off with a single PS layer using the LLL approach (Fig. 2). Once the porosity is obtained from the fitting of the spectra, the complex refractive index may be calculated as a function of the wavelength, obtaining a plot similar to the one shown in Fig. 3b.

The program used to simulate a non modified multilayer requires as input parameters the porosities and thicknesses of the stacked layers. In the case of a modified multilayer the input parameters are the complex refractive index as a function of the energy as well as the thickness of each layer of the stack. The complex refractive index is obtained from the fitting of reflectance measurements of modified single layers, as it was previously described.

Fig. 4 shows the calculated reflectance spectrum (dotted line) corresponding to an optical microcavity centered at 700 nm composed of non modified layers, with a defect with optical thickness equal to $\lambda_c/2$. The election of this wavelength for a hypothetical biosensor prototype is not by chance. An "optical window" in the region of the near infrared (650–900 nm) represents some advantages such as low light scattering; also, in this region light is relatively poorly absorbed by biomolecules and so can penetrate deeply into the structures.

The spectrum has been evaluated with the previously described simulation program. The simulation considers the alternation of a high (128 mA $cm^{-2}$) and a low (12.4 mA $cm^{-2}$) current density during the anodization process. The porosity obtained from the fitting of the corresponding single layer reflectance was 86% and 54%, respectively, for these currents. The complex refractive index was calculated using these porosities in Eq. (1). The real part of the index evaluated at 700 nm were $n_H = 1.26$ (high current layers) and $n_L = 2.16$ (low current layers). Fig. 4 also shows the experimental reflectance spectrum (solid line) obtained for the designed multilayer. A scheme of the multilayer is shown in this figure. The anodization times for the high and the low current layers were interpolated from a plot similar to the one shown in Fig. 3c, resulting in 2.5 and 12 s for the high and the low current layers, respectively. It can be observed from Fig. 4 that the use of our simulation programs allows designing and predicting the optical response of the non modified multilayer with high accuracy.

### 4.1. Assessment of layer modification

For biosensing applications, the PS material must be functionalized in order to allow the incorporation of specific recognition elements. As a first step, the procedure implies the preparation of a multilayer with specific combination of currents and times for the anodization process. Afterwards, the surface of the porous structure is

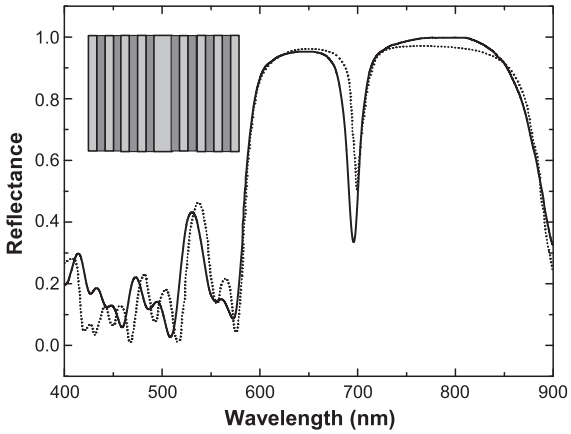


**Fig. 4.** Measured and simulated reflectance spectra of a microcavity centered at 700 nm obtained alternating high and low current densities during the corresponding times (2.5 s at 128 mA $cm^{-2}$ and 12 s at 12.4 mA $cm^{-2}$), as determined from the curves of Fig. 2. The simulated spectrum was obtained using data of complex refractive indexes inferred from measurements of single layers. The inset shows a schematic representation of a transversal view of the microcavity. The different gray tonalities correspond to different refractive index.

modified by exposing the external surface of the multilayer to the chosen chemicals. This process signifies that the chemicals must penetrate in depth the porous structure until the whole structure is completely exposed. In order to study possible effects of non-uniform modification, the simulation program employed in the prediction of multilayer response was used to reproduce the spectra resulting when only a limited number of layers were modified, those nearest to the surface. Instead of having a multilayer composed by layers of two given refractive index, we model the incorporation of the modifying agent by considering that the refractive index changes progressively along the successive layers. The non homogeneous change in the refractive index is in turn represented within this simplified model by a non homogeneous change in the porosity of the multilayer.

Fig. 5 shows the simulation results for the reflectance of an 18 layers system consisting of two Bragg mirrors with 8 layers (4 pairs of $n_H n_L$) separated by a defect of a $\lambda_c/2$. The figure shows a simulated spectrum of the non-modified microcavity together with two simulated spectra corresponding to partial modifications, and one with the whole system homogeneously modified. Several characteristics can be analyzed and used as criteria to evaluate the system modification by comparing the measured spectrum of the microcavity with the simulated ones resulting from modification of different number of layers. In the simulated spectra of the in depth non-uniformly modified multilayer, in which only the first near-surface layers were modified (7 layers), the shape of the stopping band changes, and the resonance peak shifts only by few nanometers with respect to the unmodified structure. The deformation of the stopping band increases when the number of modified layers goes up, as it can be observed in Fig. 5 for the spectrum corresponding to seven modified layers, a sample in which the modification almost reaches the cavity. When the modification involve a larger number of layers, going over the cavity defect, the resonance shifts close to the final location, muddling up with the case of uniform modification (case in which the modification reaches the 18 layers). However, unlike the case of uniform modification, the spectrum with an almost complete modification has larger side lobes. This is the case in which up to 12 layers are modified (see Fig. 5).

Also, it is worth noting that the reflectance is not zero and presents undulations on both sides of the stopping band. These undulations are the so called “side lobes”. The relative heights of the side lobes of the non-uniformly modified or partially modified in depth samples are higher in the zone of shorter wavelengths and lower in the zone of longer wavelengths than those of the non-modified sample. Thus, for example, the non-modified microcavity present a side lobe with double band centered at around 475 nm, that shifts almost without deformation, in the case of the uniformly modified sample to 540 nm, maintaining its shape. When the multilayer is partially modified in depth (cases of 7 and 12 layers in Fig. 5), the side lobe become a higher single peak centered at 530 and 550 nm for the case of 7 and 12 modified layers, respectively. In the same way, the heights of side lobe longer wavelengths of the non-modified and uniformly modified multilayers are similar. On the contrary, the large wavelengths side lobes are smaller in the cases of partially modified multilayers.

Fig. 6 shows the reflectance spectra for a freshly etched PS (solid line) and after the silanization by the one step modification procedure (dotted line). Even though the whole spectrum shifts to longer wavelengths as previously mentioned, a closer examination of the resonance peak and side lobes shows that the spectrum features are not preserved as it is expected for a homogeneously modified sample (at shorter wavelengths than the resonance, the side lobes of the non-modified sample is a double structured peak whose maximums have a great difference in height, while for the modified samples the maximums have almost the same height). In the experimental conditions used for this one step method, a low reproducibility was observed; the bandwidth peak of most of the samples increases (see inset in Fig. 6), probably due to the degradation of the porous structure by the alkaline conditions. Instead, for the samples modified using the two step procedure, a blue shift can be observed after the oxidation step. In the second step, when the silane radicals are incorporated, the whole spectrum shifts to longer wavelengths. The shifts occur preserving the main features of the spectrum (Fig. 7). In the first step, a blue shift of the resonance of $22 \pm 4$ nm can be observed, and for the silanization step the red shift was $13 \pm 3$ nm. It is worth to note in Fig. 7 that the whole spectrum is displaced without changing its shape. The resonance shifts with the whole spectrum and the side lobes at both sides of the resonance band are almost preserved in shape and height. Taking into account the results of simulations, these features strongly suggest that the modification occurs uniformly in all the layers of the multilayer.

## 5. Conclusions

Our results show that computational codes can help to rationally design porous silicon multilayers for sensor applications. The procedure implies the determination of the optical properties of porous silicon single layers using reflectance measurements. The process concludes with the simulation of the spectral response of the desired multilayer using the optical properties previously determined. The method may be applied to freshly prepared layers as well as to

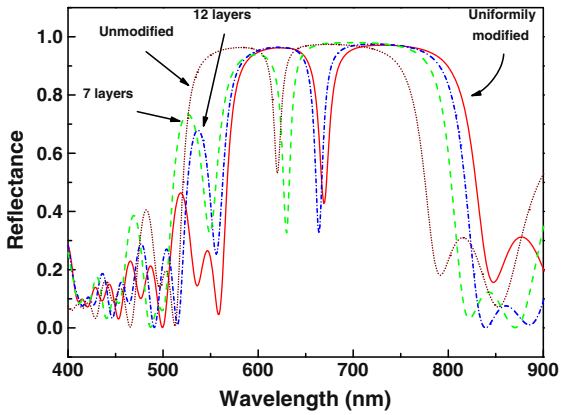


**Fig. 5.** Results of the simulated reflectance spectra of an unmodified (doted line) and uniformly modified (solid line) optical microcavity. The spectra corresponding to partial modifications, for 7 (dashed line) and 12 (dash–doted line) layers modification, are also shown (see text for details).

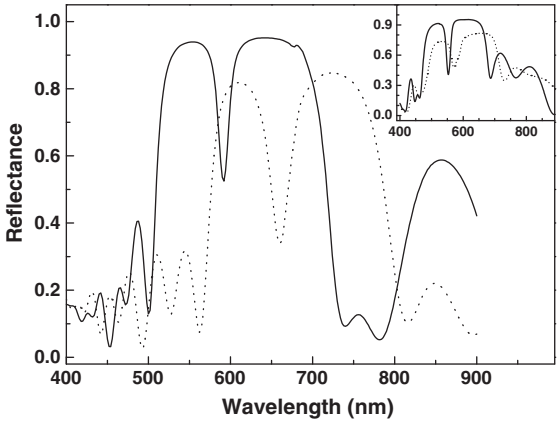


**Fig. 6.** Measured spectra of an optical microcavity: freshly etched PS sample (solid line), and after modification (dotted line) by the one step procedure. The inset of the figure shows the result obtained for a similar sample treated with the same procedure. The result demonstrates the lack of reproducibility for this method.

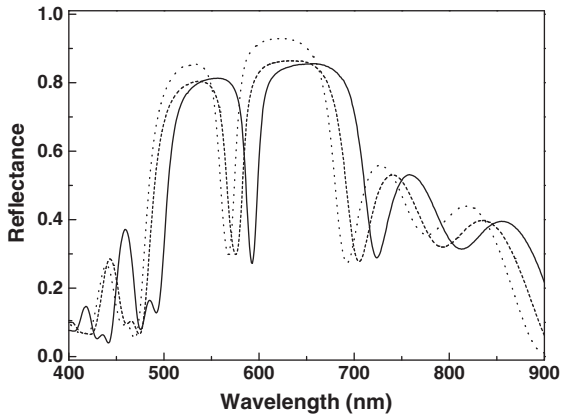


**Fig. 7.** Measured spectra of an optical microcavity: freshly etched PS sample (solid line), the same sample oxidized by hydrogen peroxide (dotted line), and the same sample after silanization (dashed line) by the two step modification. The shift of the spectrum as a whole without appreciable modifications, including the features corresponding to the resonance and side lobes, strongly suggest uniform modification as inferred from the simulations shown in Fig. 4.

functionalized layers. The simulation procedure allows distinguishing among homogenously modified and partially modified samples showing that the computational codes are a useful tool to analyze and track the modification steps of the multilayers in PS sensors. Optical responses of both structures were compared giving a conclusion on quality of each derivatization method. Thus, comparing experimental results with the numerical model, it was shown, that the porous structure is uniformly modified in depth when samples were oxidized with hydrogen peroxide and then modified by the silanization reaction with APTES.

## Acknowledgments

This work has been supported by the ANPCyT under project Prestamo BID PICT 32515 and PICT 00575, and by the Universidad Nacional del Litoral under project CAI + D 2009 N° 68–343.

## References

[1] V.-Y. Lin, K. Motesharei, K.S. Dancil, M.J. Sailor, M.R. Ghadiri, Science 278 (1997) 840.
[2] M. Archer, M. Christophersen, P.M. Fauchet, Sens. Actuators B: Chem. 106 (2005) 347.
[3] A. Jane, R. Dronov, A. Hodges, N.H. Voelcker, Trends Biotechnol. 27 (2009) 230.
[4] O. Bisi, S. Ossicini, L. Pavesi, Surf. Sci. Rep. 38 (2000) 1.
[5] H. Föll, M. Christophersen, J. Carstensen, G. Hasse, Mater. Sci. Eng. R 39 (2002) 93.
[6] A. Janshoff, K.-P.S. Dancil, C. Steinem, D.P. Greiner, V.S.-Y. Lin, C. Gurtner, K. Motesharei, M.J. Sailor, M.R. Ghadiri, J. Am. Chem. Soc. 120 (1998) 12108.
[7] M.P. Stewart, J.M. Buriak, Adv. Mater. 12 (12) (2000) 859.
[8] G.T. Hermanson, Bioconjugate Techniques, Academic Press, Elsevier Science, USA, 1996.
[9] W. Theiss, Surf. Sci. Rep. 29 (1997) 91.
[10] J.E. Spanier, I.P. Herman, Phys. Rev. B 61 (2000) 10437.
[11] In: S. Kasap, P. Kapper (Eds.), Spinger Handbook of Electronic and Photonic Materials, Spinger, Canada, 2006.
[12] V. Torres-Costa, R.J. Martín-Palma, J.M. Martínez-Duart, J. Appl. Phys. 96 (2004) 4197.
[13] M. Born, E. Wolf, Principles of Optics, 6th ed. Pergamon Press, Oxford, 1980.
[14] Hong-Liang Li, Ai-Ping Fu, Dong-Sheng Xu, Guo-Lin Guo, Lin-Lin Gui, You-Qi Tang, Langmuir 18 (2002) 3198.
[15] U. Frotscher, U. Rossow, M. Ebert, C. Pietryga, W. Richter, M.G. Berger, R. Arens-Fischer, H. Munder, Thin Solid Films 276 (1996) 36.
[16] David E. Goldberg, Genetic Algorithms in Search, Optimization, and Machine Learning, Addison-Wesley, Reading, Massachusetts, 1989.
[17] J.C. Lagarias, J.A. Reeds, M.H. Wright, P.E. Wright, SIAM J. Optim. 9 (1) (1998) 112.
[18] R. Urteaga, O. Marín, L.N. Acquaroli, D. Comedi, J.A. Schmidt, R.R. Koropecki, J. Phys. Conf. Ser. 16 (7) (2009) 012005.